

## L-H Transition Studies on DIII-D to Determine H-mode Access for Operational Scenarios in ITER

P. Gohil<sup>1</sup>, T.E. Evans<sup>1</sup>, M.E. Fenstermacher<sup>2</sup>, J.R. Ferron, D.C. McDonald<sup>3</sup>, T.H. Osborne<sup>1</sup>,  
J.M. Park<sup>4</sup>, O. Schmitz<sup>5</sup>, J.T. Scoville<sup>1</sup> and E.A. Unterberg<sup>4</sup>

<sup>1</sup>General Atomics, P.O. Box 85608, San Diego, California 92186-5608, USA

<sup>2</sup>Lawrence Livermore National Laboratory, Livermore, California 94550, USA

<sup>3</sup>Euratom/CCFE Fusion Association, Culham Science Center, Abingdon, OX14 3DB, UK

<sup>4</sup>Oak Ridge National Laboratory, Oak Ridge, Tennessee 37831, USA

<sup>5</sup>Forschungszentrum Jülich GmbH, IEF4-Plasma Physics, 52428 Jülich, Germany

e-mail: gohil@fusion.gat.com

**Abstract.** A comprehensive set of L-H transition experiments has been performed on DIII-D to determine the requirements for access to H-mode plasmas in ITER's first (non-nuclear) operational phase with H and He plasmas and the second (activated) operational phase with D plasmas. The H-mode power threshold,  $P_{\text{TH}}$ , was evaluated for different operational configurations and auxiliary heating methods for the different main ion species. Helium plasmas have significantly higher  $P_{\text{TH}}$  than deuterium at low densities for all heating schemes, but similar  $P_{\text{TH}}$  as deuterium at high densities except for H-neutral beam injected heated discharges, which are still higher. Changes in  $P_{\text{TH}}$  are observed when helium concentration levels in deuterium plasmas exceed 40%. There is a strong dependence of  $P_{\text{TH}}$  on the magnetic geometry in the vicinity of the divertor. The trend of decreasing  $P_{\text{TH}}$  with decreasing X-point height is observed for all the main ion species irrespective of the heating method, which appears to indicate that there is a common physics process behind this effect for all the ion species. Helium and deuterium exhibit a significant increase in  $P_{\text{TH}}$  for strong resonant magnetic perturbations. The application of a local magnetic ripple of 3% from test blanket module mock-up coils did not change  $P_{\text{TH}}$  in deuterium.

### 1. Introduction

High levels of fusion power production in future magnetic fusion devices, such as ITER, will be dependent on achieving high values of energy confinement and plasma pressure at the device operating plasma parameters. An extensive set of L-H transition experiments has recently been performed on DIII-D to determine the requirements for access to H-mode plasmas in ITER's first (non-nuclear) operational phase with H and He plasmas, and second (activated) operational phase with D plasmas. Earlier studies of the H-mode power threshold in hydrogen and helium on other magnetic fusion devices [1–4] have revealed significantly higher H-mode power thresholds compared to those in deuterium. More recent studies on DIII-D showed higher H-mode threshold powers for hydrogen and helium than for deuterium [5–7]. This is in contrast with recent results from ASDEX Upgrade that showed that the H-mode power threshold was the same for helium and deuterium [8]. Given the large variation in these results for different ion species, a systematic set of experiments was performed on DIII-D to elucidate the H-mode power threshold dependences for the different ion species on: (1) the L-mode electron density; (2) the helium purity; (3) different auxiliary heating methods [electron cyclotron heating (ECH), helium neutral beam injection (NBI), hydrogen NBI and deuterium NBI]; (4) the magnetic geometry at the divertor; (5) resonant magnetic perturbations; (6) the local magnetic ripple from test blanket module (TBM) mock-up coils. We describe results of these experiments expanding on previous results on hydrogen, deuterium and helium discharges presented in Refs. [6,7]. Section 2 describes the experimental setup and procedure. Succeeding sections provide details for each type of  $P_{\text{TH}}$  dependence.

### 2. Experimental Setup

The experimental setup and procedures used for the experiments described in this paper were similar to those for previous studies of the L-H transition with different main ion species and

as described in references [5–7]. The main plasma parameters for many of these experiments were plasma current,  $I_p = 1.0$  MA, toroidal magnetic field,  $B_T = 1.65$  T, safety factor,  $q_{95} = 4.1$  and a range of line-averaged densities in L-mode of  $1.5\text{--}6 \times 10^{19} \text{ m}^{-3}$ . The overall plasma geometry included major radius,  $R = 1.7$  m, minor radius,  $a = 0.6$  m, elongation,  $\kappa = 1.7$  and surface area at the plasma boundary,  $S = 56 \text{ m}^2$  with a height of the X-point above the divertor surface of 26 cm. The net power required to transition from L-mode to H-mode plasmas was measured with incremental ramps in the auxiliary heating power, such as electron cyclotron heating (ECH) power and injected neutral beam power. The presence of co- $I_p$  and counter- $I_p$  directed beams in DIII-D allows for “balanced” beam injection in which the net torque imparted to the plasma is near zero. The auxiliary power was increased in steps during the discharges by adding more ECH gyrotron power, or by adding neutral beam injection (NBI) power increments through modulation of particular beams, with the increments also depending on the accelerator voltage setting of each beam. The NBI accelerator voltage settings varied between 55 to 81 kV, and beam modulations were in 25% increments of the max duty cycle of 40 ms. Overall, this corresponded to minimum power increments of 0.2–0.4 MW depending on the beam species used. Modulation times were less than the fast-ion slowing down time. The duration of the NBI power steps was typically 320–480 ms, which corresponded to many energy confinement times (depending on the main ion species) and enabled the plasma to react to the time-averaged increases in power. The power scans for both ECH and NBI cases were initiated at a level well below the expected H-mode power threshold during the stationary L-mode phase of the discharges. NBI steps were performed at near zero torque with “balanced” beams throughout the discharge. The peak of the beam deposition profile is near the plasma center in DIII-D. Most of the discharges with ECH ( $f = 110$  GHz, radial launch, 2<sup>nd</sup> harmonic heating) had the deposition layer centered at  $r/a \sim 0.7$  ( $\pm 0.05$ ) as determined by the ECH ray tracing code, TORAY [10]. In some cases, the ECH deposition layer was changed to  $r/a \sim 0.3$  and 0.5 with no significant change in the H-mode power threshold. The net H-mode power threshold was determined from the sum of the input power [NBI, ECH, Ohmic] minus the beam shine-through and ion orbit losses, the bulk radiated power from the plasma and the time derivative of the diamagnetic energy,  $dW/dt$ . Some cases shown did not transition into H-mode with the available input power, indicating an approximate lower bound to the H-mode power threshold for those specific conditions.

### 3. Density Dependence of the Power Threshold

A minimum in the density dependence of the H-mode power threshold has been observed on many devices [11–13]. The present study sought to determine the density dependence of the power threshold for deuterium and helium and for different heating methods relevant to ITER (results in DIII-D hydrogen plasmas were previously published in [6]). Figure 1 shows the density dependence of the H-mode power threshold,  $P_{TH}$ , for deuterium and helium plasmas for NBI and ECH discharges. Figure 1(a) shows the density dependence for deuterium NBI into deuterium plasmas, helium NBI into helium plasmas and hydrogen NBI into helium plasmas. Also shown is the threshold power for deuterium plasmas from the ITPA 2008 scaling expression [9],

$$P_{TH,scal08}(D) = 0.049 B_T^{0.80} n_e^{0.72} S^{0.94} , \quad (1)$$

where  $B_T$  is the toroidal magnetic field (T),  $n_e$  is the line-averaged electron density in L-mode ( $10^{20} \text{ m}^{-3}$ ) and  $S$  is the plasma surface area ( $\text{m}^2$ ). At the lower target densities ( $< 3 \times 10^{19} \text{ m}^{-3}$ ), there are clear differences in the power threshold depending on the main ion species with deuterium plasmas having the lowest power threshold. However, at higher densities (e.g.  $\sim 4 \times 10^{19} \text{ m}^{-3}$ ) the threshold powers for deuterium and helium plasmas heated by NBI with the same species as the plasma species (i.e. D-NBI  $\rightarrow$  D and He-NBI  $\rightarrow$  He) are similar. The

power threshold for discharges with hydrogen NBI into helium plasmas is substantially higher than the above cases at all densities. However, the level of beam fueling is expected to be lower in ITER and so should lead to a lower level of hydrogen dilution than the 20%–50% seen in DIII-D. A minimum in the density dependence is observed for D-NBI  $\rightarrow$  D and He-NBI  $\rightarrow$  He discharges. Figure 1(a) indicates that the power threshold for helium plasmas in ITER should be similar to those in deuterium given operation at mid to high target densities.

Deuterium and helium discharges heated with ECH also exhibit clear minima in the density dependence of the power threshold as shown in Fig. 1(b). The minimum for helium occurs at a slightly higher density than for deuterium and the difference between  $P_{TH}$  for D and He becomes small at higher densities. NBI-heated deuterium discharges have similar  $P_{TH}$  to ECH deuterium discharges over the range of densities investigated. The  $P_{TH}$  for NBI heated He discharges is lower than ECH discharges at low densities, but higher at high densities ( $\sim 5 \times 10^{19} \text{ m}^{-3}$ ). This behavior may be related to differences in the

equi-partitioning of energy between the ions and electrons as a function of density between deuterium and helium plasmas. Overall, helium plasmas have significantly higher  $P_{TH}$  than deuterium plasmas at low densities for all heating schemes, but similar  $P_{TH}$  as deuterium plasmas at high densities except for H-NBI heated discharges, which are still higher.

#### 4. Power Threshold Dependence on Helium Purity

An experiment was performed to determine the threshold power as a function of the ratio of helium to deuterium concentration by operating with deuterium discharges after boronization of the DIII-D vessel [14]. Deuterium plasma discharges produced immediately following boronization tend to have a high helium concentration, which then decreases with subsequent discharges. The H-mode power threshold was determined for repeat identical deuterium plasma discharges (1.0 MA, 1.65 T,  $n_e = 2.8\text{--}3.0 \times 10^{19} \text{ m}^{-3}$ ) in which the helium concentration progressively decreased with increasing shot number. Each discharge was heated by an initial sequence of increasing steps in ECH power (to determine the power threshold) followed by high power deuterium NBI later in each discharge to aid in the helium cleanup process. The deuterium concentration was determined from neutron detection measurements using low power beam blips during the ECH. It was assumed that the rest of the plasma consisted of helium. Figure 2 shows how the H-mode power threshold varied with the concentration of helium in the plasma. Initially too high to enable access to H-mode, the power threshold steadily decreased shot-to-shot as the helium purity declined on subsequent shots until it approached the power threshold levels consistent with pure deuterium plasmas (i.e. about 1.2 MW), which was achieved for  $\text{He}_{\text{conc}} < 20\%$ . He concentrations exceeding 40%

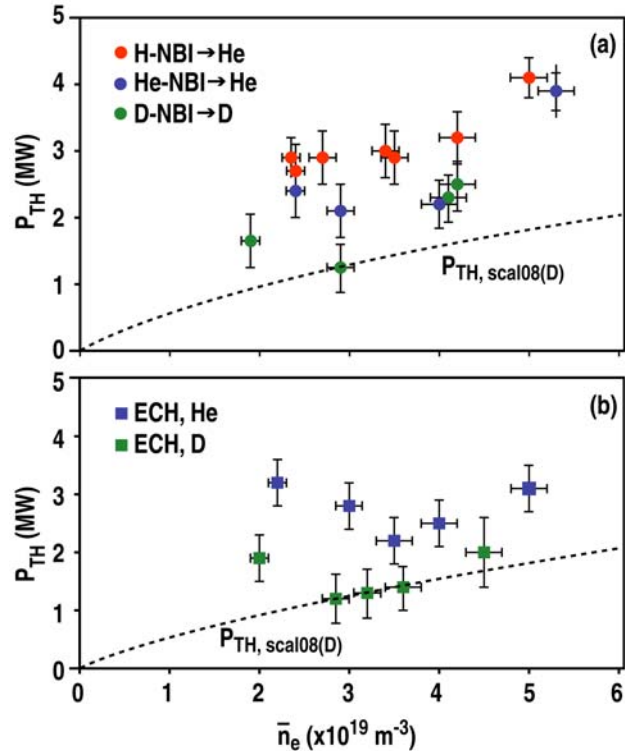


FIG. 1. The H-mode power threshold as a function of the line-integrated L-mode density for D and He plasmas (1.0 MA, 1.65 T) discharges with auxiliary heating by (a) NBI and (b) ECH. The dashed line corresponds to the power threshold scaling relation for D plasmas,  $P_{TH,scal08}$ , given in Eq. (1).

are enough to produce discernible increases in the H-mode power threshold in deuterium discharges.

### 5. Power Threshold Dependence on X-point Height

Previous studies in DIII-D with hydrogen and helium plasmas have revealed a very strong dependence of  $P_{TH}$  on the X-point height above the divertor surface for lower single null plasmas [6,7]. Near identical plasma shapes and parameters to previous studies reported in Refs. [6] and [7] were produced in recent DIII-D experiments. A sequence of discharges was carried out with a scan in the height of the X-point above the lower divertor with all other gaps between the plasma last closed flux surface and the vessel surfaces being maintained at near constant values. Figure 3 shows the temporal evolution of two EC-heated helium discharges with different X-point heights taken from this scan. The discharge with the low X-point location transitions into the H-mode at over a factor of 2 lower ECH power. Figure 4 shows that  $P_{TH}$  decreases with decreasing height of the X-point above the divertor for the different main ion species (H, D and He) and also for different heating methods (NBI or ECH). This trend in  $P_{TH}$  with the X-point height is not included in the scaling law (equation 1) and furthermore would be opposite to that described by the  $S^{0.94}$  term in the scaling law. Varying the X-point height changes both the separatrix geometry and the recycling in the vicinity of the divertor. Further experiments are required to determine the underlying physics for this variation in the H-mode power threshold.

### 6. Power Threshold Dependence on Resonant Magnetic Perturbations

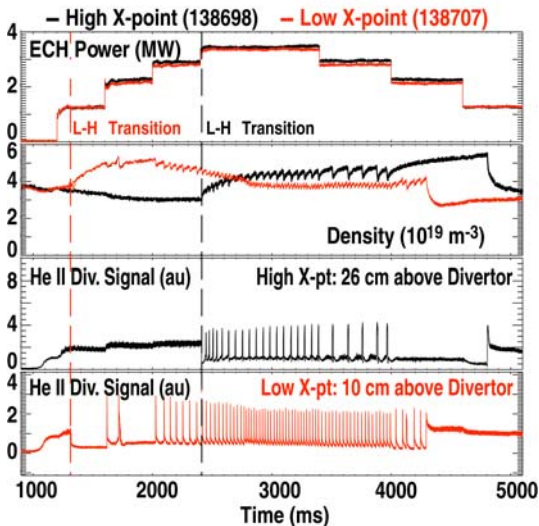


FIG. 3. Evolution of plasma variables with varying ECH power for 2 He plasma discharges (1.0 MA, 1.65 T) with different heights of the X-point with respect to the lower divertor surface.

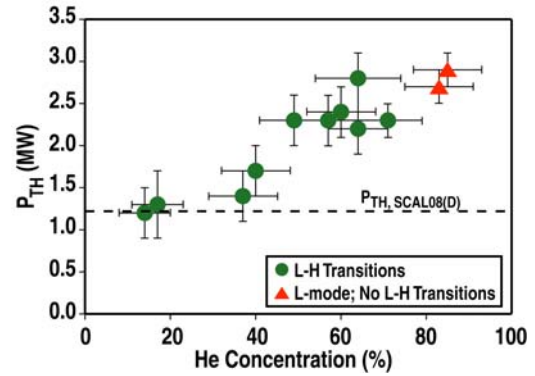


FIG. 2. The H-mode power threshold for D plasma discharges with varying amounts of He concentration (1.0 MA, 1.65 T,  $n_e = 2.8-3.0 \times 10^{19} \text{ m}^{-3}$ ) with auxiliary heating by ECH.

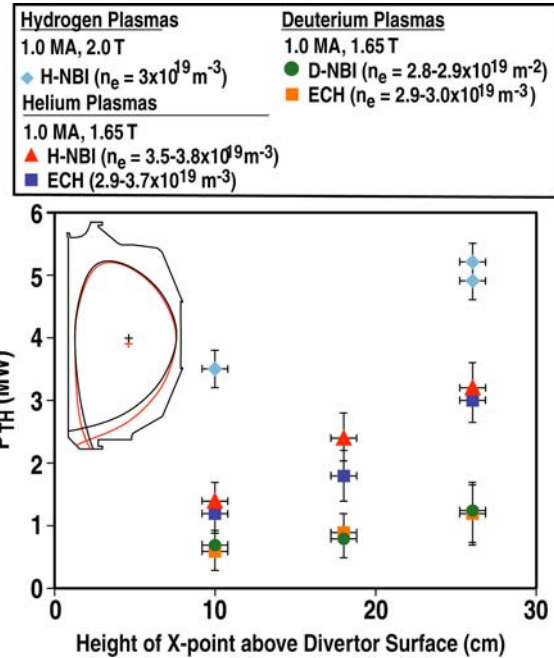


Fig. 4. The H-mode power threshold as a function of the height of the lower X-point with respect to the lower divertor surface for H, D and He plasmas and different auxiliary heating schemes. The density values in brackets correspond to the range of L-mode densities used in the scan.

### 6.1 RMP Effect on H-mode Power Threshold in Helium Plasmas

Resonant magnetic perturbations (RMPs), produced by nonaxisymmetric magnetic coils, are under consideration for control of edge localized mode (ELM) characteristics in ITER [15]. In DIII-D,  $n=3$  RMP fields are applied by in-vessel coils (I-coils) to be resonant at a specific value of  $q_{95}$ . Threshold power was assessed in the presence of these fields during ECH power ramps in helium plasmas with the standard high X-point plasma configuration. Figure 5 compares three near-identical helium plasma discharges with and without RMP fields for resonant values of  $q_{95}=3.4$  and with the applied field for the off-resonance value of  $q_{95}=4.0$ . The RMP fields were applied during the L-mode phase of the discharges. The H-mode transition was observed to occur at the lowest applied ECH power for the no-RMP case at  $q_{95}=3.4$ . The application of a current of 2 kA in the I-coils at  $q_{95}=3.4$  resulted in no transition to H-mode and the plasma remained in L-mode, with up to 3.5 MW of applied ECH. Applying the same I-coil current of 2 kA at increased  $q_{95}=4.0$  resulted in an H-mode transition at a slightly higher applied ECH power than the no I-coil case. Figure 6 shows the variation in  $P_{TH}$  as a function of the I-coil current for the ECH cases and for balanced (zero torque) H-NBI into He plasmas. An effect on  $P_{TH}$  is observed at even low I-coil currents of 1 kA in both cases. A smaller increase in  $P_{TH}$  was also observed for strong off resonance fields ( $q_{95}\sim 4.0$ ).

### 6.2 RMP Effect on H-mode Power Threshold in Deuterium Plasmas

Experiments were also performed to determine how RMPs affect  $P_{TH}$  in deuterium plasmas in preparation for the D-D phase of ITER operations. Again, the application of RMPs led to increases in the

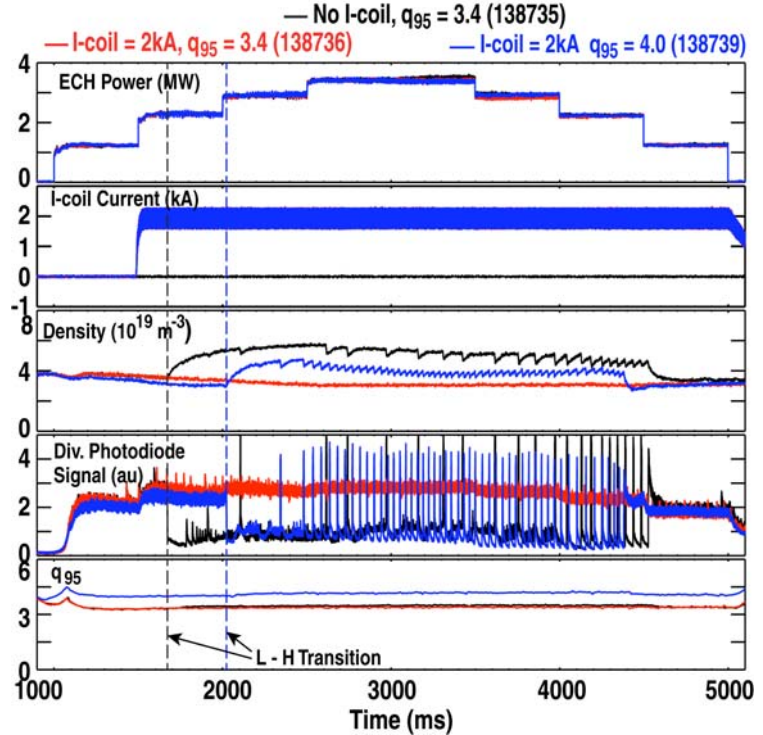


FIG. 5. Evolution of line averaged density, divertor He II emission and edge safety factor,  $q_{95}$ , for He discharges with varying ECH power and different I-coil currents (0, 2 kA). The plasma discharges are operated at 2 nominal values of  $q_{95}$  (3.4, 4.0).

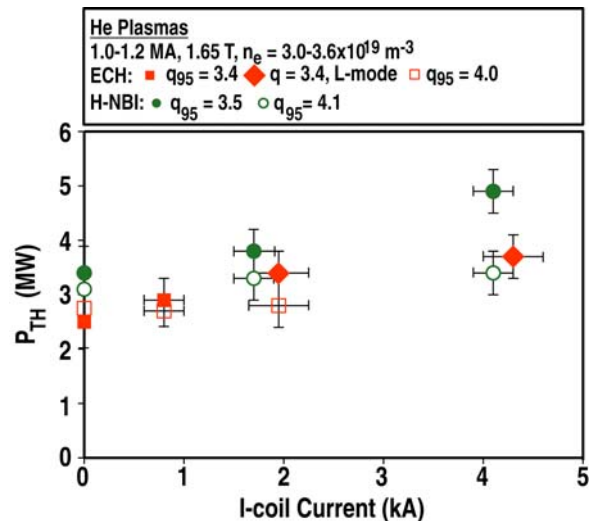


FIG. 6. The H-mode power threshold as a function of I-coil current for He plasmas and different values of edge safety factor,  $q_{95}$ . The plasmas are heated by ECH or H-NBI. All the discharge transitioned to H-mode at the lowest power indicated except for the red diamond data points, which remained in L-mode at the available ECH power.

H-mode power threshold. These experiments



were performed with the ITER similar shape (ISS) used for many of the experiments involving ELM suppression by RMP on DIII-D [16] (different from that used for the helium plasmas). The power threshold experiments were performed using ECH and balanced D-NBI into pure deuterium plasmas (1.1–1.3 MA, 1.7 T,  $n_e=2.7\text{--}3.1\times 10^{19}\text{ m}^{-3}$ ,  $q_{95}=3.4\text{--}4.0$ ). Figure 7 shows two identical deuterium plasma discharges with balanced D-NBI: one with no I-coil current and the other with an I-coil current of over 4 kA. The discharges had  $q_{95}=3.4$  to be in the resonant window for the RMP field. The I-coil current was initiated during the L-mode phase of the discharge and held constant for over 2 seconds. The NBI power was stepped up with net zero torque-balanced beams during the duration of NBI. The NBI power required to transition to the H-mode was clearly higher in the discharge with the I-coil current on. The line-averaged density in H-mode was lower during the application of the I-coil current as a result of density “pump-out” by the RMP field. Figure 8 compares H-mode power thresholds for different I-coil currents. The solid green circles correspond to the NBI heated discharges at  $q_{95}=3.4$ , which were resonant with the RMP field and that transitioned to H-mode. The discharge with the highest I-coil current of 5.3 kA did not transition to L-mode at that applied NBI power. The open green circles correspond to NBI heated discharges with off resonant components (i.e. at  $q_{95}=4.0$ ) that transitioned to H-mode. The  $P_{\text{TH}}$  for ECH discharges with resonant  $q_{95}$  values are depicted by the red solid squares and off resonant values by the open red squares. The ECH discharge at I-coil current of 3.3 kA denoted by a red solid triangle did not transition to H-mode with the available ECH power. Overall, for strong resonant components in the RMP spectrum, there is a significant increase in  $P_{\text{TH}}$  for RMP fields above a critical threshold field (i.e. for I-coil currents above 3 kA), whereas no clear increase is observed below this field level. For non-resonant fields, there is a much smaller increase in  $P_{\text{TH}}$  with the applied field. I-coil currents between 4–7 kA are normally required for ELM suppression [16,17]. Results from similar power threshold studies in NSTX and MAST indicate similar increases in  $P_{\text{TH}}$  with strongly resonant RMP

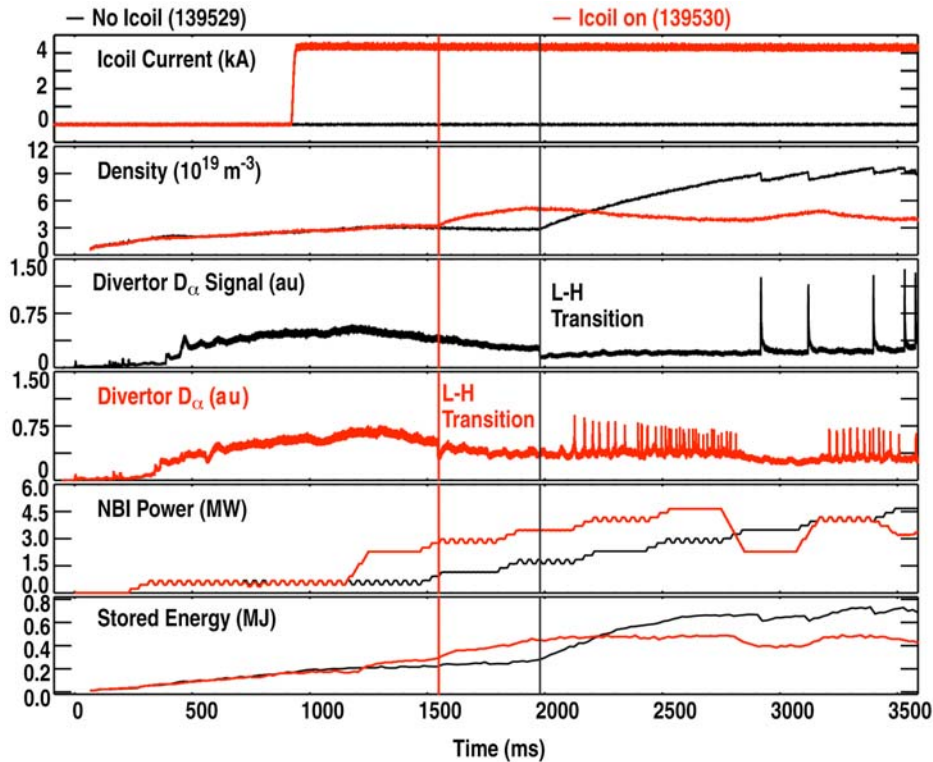


FIG. 7. Evolution of the line averaged density, divertor  $D_\alpha$  emission and diamagnetic energy for D discharges (1.3 MA, 1.7 T) with varying deuterium NBI, with and without the application of I-coil current (0, 4.3 kA).

fields above a threshold field [18]. Helium plasmas do not exhibit a clear threshold in the RMP field strength for increases in  $P_{TH}$  since the  $P_{TH}$  is observed to increase at even very low I-coil currents.

### 7. Effect of Local Magnetic Ripple From Test Blanket Module on Power Threshold

A key ITER goal is to evaluate tritium-breeding TBMs during the nuclear operational phase. Three pairs of ferromagnetic TBMs are planned to be installed on ITER. The presence of these large masses (~1.3 tonne per TBM) of ferromagnetic material will introduce appreciable amounts of local magnetic ripple [toroidal field (TF) + TBM ripple ~1.3%] in the vicinity of the TBMs. In order to determine if these levels of magnetic ripple would affect the H-mode power threshold, an experiment was performed on DIII-D using a set of coils to produce local toroidal and poloidal fields to mock up more than 3 times the field that would be induced in one pair of TBMs in ITER [19]. The experiment was performed with a plasma configuration different from those described in the previous sections and which would be compatible for performing other plasma evaluations (e.g. plasma performance in H-mode, effects on plasma rotation and mode locking, etc.) using the coils. Deuterium plasmas were investigated with ECH, balanced D-NBI and co-directed D-NBI. A TF+TBM local ripple of 3% was applied using the mock-up coils during the L-mode phase of each heating scheme. Figure 9 shows the H-mode power threshold as a function of input torque for plasmas with and without the TBM mock-up coils energized. Very slight increases in  $P_{TH}$  are observed near zero torque, but are well within the error bars of the measurements, indicating no significant change in  $P_{TH}$  for the applied local ripple of 3%.

### 8. Summary and Conclusions

A comprehensive set of L-H transition experiments has been performed on DIII-D to determine the requirements for access to H-mode in ITER's first (non-nuclear) operational phase with H and He plasmas and second (activated) operational phase with D plasmas. The goal of these experiments was to evaluate the H-mode power threshold dependences for the different main ion species on: (1) the L-mode electron density; (2) the helium purity; (3) different auxiliary heating methods [electron cyclotron heating (ECH), helium NBI, hydrogen NBI and

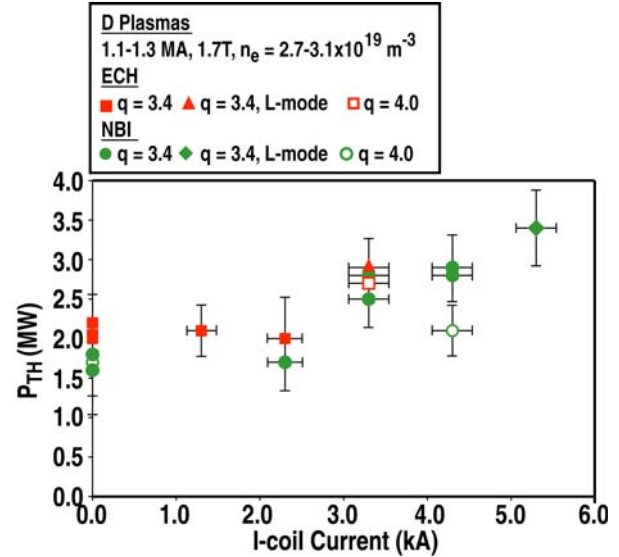


FIG. 8. H-mode power threshold as a function of the I-coil current for D plasmas and different values of edge safety factor,  $q_{95}$ . The plasmas are heated by ECH or D-NBI.

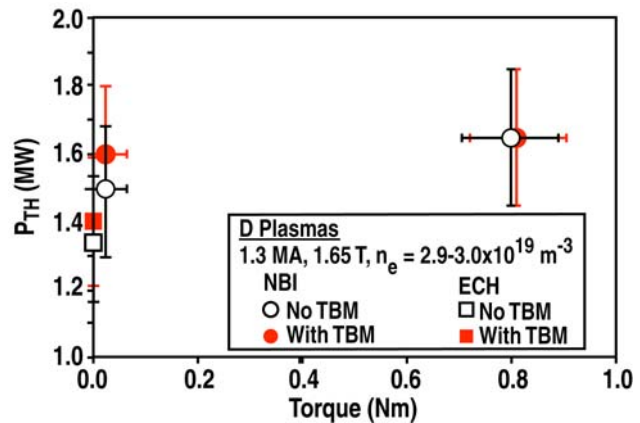


FIG. 9. H-mode power threshold as function of input torque for D plasmas with and without the application of current through coils which mock-up the magnetic fields expected from TBMs in ITER. The data points with the TBM correspond to the application of a local (TF+TBM) magnetic ripple of 3%. Auxiliary heating consists of ECH, balanced D-NBI or co-NBI.

deuterium NBI]; (4) the magnetic geometry at the divertor; (5) resonant magnetic perturbations; (6) the local magnetic ripple from TBM mock-up coils.

The difference in the power threshold between deuterium and helium plasmas is density dependent. Helium plasmas have significantly higher  $P_{\text{TH}}$  than deuterium plasmas at low densities for all heating schemes, but similar  $P_{\text{TH}}$  as deuterium plasmas at high densities except for H-NBI heated discharges, which are still higher. Changes in  $P_{\text{TH}}$  are observed when helium concentration levels in deuterium plasmas exceed 40%. The power threshold in NBI heated discharges is similar to ECH discharges for nearly all densities in deuterium plasmas, whereas helium plasmas exhibit lower  $P_{\text{TH}}$  with NBI than ECH at low densities, but higher  $P_{\text{TH}}$  for NBI at higher densities. There is a strong dependence of  $P_{\text{TH}}$  on the divertor X-point height. Decreasing  $P_{\text{TH}}$  with decreasing X-point height is observed for all the main ion species irrespective of the heating method, suggesting a common physics process behind this effect for all the ion species. Helium and deuterium plasmas exhibit a significant increase in  $P_{\text{TH}}$  for strong resonant components in the RMP spectrum. For D plasmas, there is a significant increase in  $P_{\text{TH}}$  for RMP fields above a critical threshold field, whereas no clear increase is observed below this field level. Based on these results, ELM control coils in ITER should likely be energized after the H-mode transition, but before the first type 1 ELM. The application of a local magnetic ripple of 3% from TBM mock-up coils did not change  $P_{\text{TH}}$  in deuterium plasmas. The presence of TBMs is therefore not expected to strongly affect the H-mode power threshold for deuterium plasmas in ITER.

This work was supported in part by the US Department of Energy under DE-FC02-04ER54698, DE-AC52-07NA27344, and DE-AC05-00OR22725.

## References

- [1] LACKNER, K., *et al.*, Plasma Phys. Control. Fusion **36** (1994) B79
- [2] RYTER, F. and the H-Mode Database Working Group, Nucl. Fusion **36** (1996) 1217
- [3] RIGHI, E., *et al.*, Nucl. Fusion **39** (1999) 309
- [4] McDONALD, D.C., *et al.*, Plasma Phys. Control. Fusion **46** (2004) 519
- [5] GOHIL, P., *et al.*, J. of Physics: Conf. Series **123** (2008) 012017
- [6] GOHIL, P., *et al.*, Nucl. Fusion **49** (2009) 115004
- [7] GOHIL, P., *et al.*, Nucl. Fusion **50** (2010) 064011
- [8] RYTER, F., *et al.*, Nucl. Fusion **49** (2009) 062003
- [9] MARTIN, Y.R., *et al.*, J. of Physics: Conf. Series **123** (2008) 012033
- [10] LIN-LIU, Y.R., *et al.*, Phys. Plasmas **10** (2003) 4064
- [11] FUKUDA, T., *et al.*, Nucl. Fusion **37** (1997) 1199
- [12] HUBBARD, *et al.*, Plasma Phys. Control. Fusion **40** (1998) 689
- [13] ANDREW, Y., *et al.*, Nucl. Fusion **48** (2006) 479
- [14] PHILIPS, J., *et al.*, J. Vac. Sci. Technol. **A10** (1992) 1252
- [15] ITER Physics Basis Editors, Nucl. Fusion **47** (2007) S1
- [16] EVANS, T.E., *et al.*, Phys. Plasmas **13** (2006) 056121
- [17] EVANS, T.E., *et al.*, Nucl. Fusion **48** (2008) 024002
- [18] FENSTERMACHER, M.E., *et al.*, this conference, ITR/P1-30
- [19] SCHAFFER, M.J., *et al.*, this conference, ITR/1-3